Microstructural Changes in SDS Micelles Induced by Hydrotropic Salt

P. A. Hassan,† Srinivasa R. Raghavan,‡ and Eric W. Kaler*

Center for Molecular and Engineering Thermodynamics, Department of Chemical Engineering, University of Delaware, Newark, Delaware 19716

Received September 13, 2001. In Final Form: January 4, 2002

The addition of low concentrations of the hydrotropic salt *p*-toluidine hydrochloride (PTHC) to solutions of the anionic surfactant sodium dodecyl sulfate (SDS) promotes the transition from spherical to rodlike micelles. NMR measurements confirm that the hydrotrope adsorbs at the micelle−water interface, thereby screening electrostatic repulsions between the surfactant headgroups. The sphere-to-rod transition in dilute solutions is followed using quasielastic light scattering, and in the semidilute concentration range dynamic rheology is used to probe the viscoelastic nature of the solutions. The scaling of the zero-shear viscosity and the plateau modulus with surfactant concentration indicates the presence of electrostatic interactions between the micelles.

Introduction

The addition of inorganic or organic salts to an ionic surfactant solution facilitates the transition from spherical to rodlike micelles by screening the repulsions between the charged headgroups.[1−7] Inorganic counterions (e.g., Cl^-, Br^-) bind moderately to cationic micelles and thus lead to gradual micellar growth, with the molar ratio of salt to surfactant typically above 1. Organic counterions that bind strongly to the micellar surface are highly efficient in promoting micellar growth[8−10] and induce wormlike micelles at significantly lower ratios of salt to surfactant.

Typical "binding" counterions for cationic micelles include salicylate,[11,12] *p*-toluene sulfonate,[13] chlorobenzoate,[14] hydroxy naphthalene carboxylate,[15,16] and alkyl sulfates.[17] Most of these additives belong to the family of *hydrotropes*,[18] i.e., weakly surface-active compounds that can increase the solubility of organic substances in aqueous solution. These counterions interact with the micelle-forming surfactant electrostatically as well as hydrophobically, and the orientation of the hydrophobe at the micellar surface is important. For example, NMR measurements show that the salicylate ion is strongly adsorbed to cetyl trimethylammonium bromide micelles in a configuration that allows the carboxylic and hydroxyl groups to protrude from the micelle.[19] The ortho isomer, salicylate, is more effective than other isomers of hydroxy benzoates in driving micellar growth.[20]

Wormlike micelles formed by cationic surfactants upon addition of hydrotropic salts such as sodium salicylate have been studied extensively.[8,21] These micelles can grow as long as several microns, with radii of typically 2−3 nm.[22] The presence of such supramolecular structures imparts strong viscoelasticity to the solution, and the rheology of these fluids is similar to that of solutions of flexible polymers. However, because the micelles are in dynamic equilibrium with their monomers, they can break and recombine rapidly and thus are called "living polymers".[8,21] Cates and co-workers have described the linear and nonlinear viscoelastic properties of such wormlike micellar solutions on the basis of a modified reptation model incorporating the effect of reversible scission kinetics.[23]

Whereas hydrotrope effects for cationic surfactants have been studied extensively, there are few reports of analogous effects for anionic surfactants. Anionic wormlike micelles have been reported mainly in the presence of high concentrations of hydrated salts (e.g., 0.6 M NaCl) or upon the addition of a cationic surfactant.[24,25] We believe

* To whom correspondence should be addressed. E-mail: kaler@che.udel.edu. Tel.: (302) 831-3553. Fax: (302) 831-6751.

† Permanent address: Novel Materials & Structural Chemistry Division, Bhabha Atomic Research Centre, Mumbai 400 085, India.

‡ Permanent address: Department of Chemical Engineering, University of Maryland, College Park, MD 20742.

(1) Mazer, N. A.; Benedek, G. B.; Carey, M. C *J. Phys. Chem.* **1976**, *80*, 1075.

(2) Hoffmann, H.; Rehage, H.; Platz, G.; Schorr, W.; Thurn, H.; Ulbricht, W. *Colloid Polym. Sci.* **1982**, *260*, 1042.

(3) Porte, G.; Appell, J. *J. Phys. Chem.* **1981**, *85*, 2511.

(4) Kern, F.; Lemarechal, P.; Candau, S. J.; Cates, M. E. *Langmuir* **1992**, *8*, 437.

(5) Khatory, A.; Lequeux, F.; Kern, F.; Candau, S. J. *Langmuir* **1993**, *9*, 1456.

(6) Aswal, V. K.; Goyal, P. S.; Thiyagarajan, P. *J. Phys. Chem. B* **1998**, *102*, 2469.

(7) Aswal, V. K.; Goyal, P. S. *Phys. Rev. E* **2000**, *61*, 2947.

(8) Rehage, H.; Hoffmann, H. *Mol. Phys.* **1991**, *74*, 933.

(9) Buwalda, R. T.; Stuart, M. C. A.; Engberts J. B. F. N. *Langmuir* **2000**, *16*, 6780.

(10) Ait Ali, A.; Makhloufi, R. *Colloid Polym. Sci.* **1999**, *277*, 270.

(11) Rehage, H.; Hoffmann, H. *J. Phys. Chem.* **1988**, *92*, 4712.

(12) Ait Ali, A.; Makhloufi, R. *Phys. Rev. E* **1997**, *56*, 4474.

(13) Soltero, J. F. A.; Puig, J. E. *Langmuir* **1996**, *12*, 2654.

(14) Carver, M.; Smith, T. L.; Gee, J. C.; Delichere, A.; Caponetti, E.; Magid, L. J. *Langmuir* **1996**, *12*, 691.

(15) Hassan, P. A.; Candau, S. J.; Kern, F.; Manohar, C. *Langmuir* **1998**, *14*, 6025.

(16) Mishra, B. K.; Samant, S. D.; Pradhan, P.; Mishra, S. B.; Manohar, C. *Langmuir* **1993**, *9*, 894.

(17) Oda, R.; Narayanan, J.; Hassan, P. A.; Manohar, C.; Salkar, R. A.; Kern, F.; Candau, S. J. *Langmuir* **1998**, *14*, 4364.

(18) Balasubramanian, D.; Srinivas, V.; Gaikar, V. G.; Sharma M. M. *J. Phys. Chem.* **1989**, *93*, 3865.

(19) Manohar, C.; Rao, U. R. K.; Valaulikar, B. S.; Iyer R. M. *J. Chem. Soc., Chem. Commun.* **1986**, *5*, 379.

(20) Valaulikar, B. S.; Mishra, B. K.; Bhagwat, S. S.; Manohar, C. *J. Colloid. Interface Sci.* **1991**, *144*, 304.

(21) Cates, M. E.; Candau, S. J. *J. Phys. Condens. Matter* **1990**, *2*, 6869.

(22) Clausen, T. M.; Vinson, P. K.; Minter, J. R.; Davis, H. T.; Talmon, Y.; Miller, W. G. *J. Phys. Chem.* **1992**, *96*, 474.

(23) Cates, M. E. *Macromolecules* **1987**, *20*, 2289.

(24) Magid, L. J.; Li, Z.; Butler, P. D. *Langmuir* **2000**, *16*, 10028 and references therein.

(25) Barker, C. A.; Saul, D.; Tiddy, G. J. T.; Wheeler, B. A.; Willis, E. *J. Chem. Soc., Faraday Trans. I* **1974**, *70*, 154.

10.1021/la011435i CCC: $22.00
Published on Web 02/23/2002

Scheme 1. Structure of *p*-Toluidine Hydrochloride (PTHC)

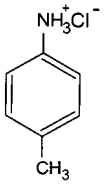

that the present study is the first example of hydrotrope-induced micellar growth in anionic surfactant solutions. The hydrotrope considered here is an aromatic salt, *p*-toluidine hydrochloride (PTHC), which features a hydrophobic cation that can bind strongly to anionic micelles (Scheme 1). We focus on the growth of sodium dodecyl sulfate (SDS) micelles in water as a function of added PTHC concentration. The orientation of the hydrotropic counterions on SDS micelles is monitored by ^{1}H NMR spectroscopy. A variety of techniques including quasielastic light scattering (QLS), capillary viscometry, and rheology is used to characterize the micelles.

Experimental Section

Materials and Methods. Sodium dodecyl sulfate (electrophoresis grade) was purchased from Fisher Scientific, and *p*-toluidine hydrochloride was obtained from Aldrich. All chemicals were used as received. Stock solutions of SDS and PTHC were prepared in deionized water and mixed in varying ratios. For light scattering measurements, the solutions were filtered through 0.2-μm nitrocellulose filters (Acrodisc) and flame sealed in 2-mL ampules. The sealed ampules were kept at room temperature for 1 day for equilibration.

Quasielastic Light Scattering (QLS). QLS measurements were made using a Brookhaven instrument with a BI200SM goniometer and a BI9000AT digital correlator. The light source was a Lexel argon ion laser operated at an output power of 100 mW at 488 nm. The scattering ampules were immersed in an index-matching fluid thermostated at 25 °C. The average decay rate was obtained from the measured autocorrelation function using the method of cumulants employing a quadratic fit. The magnitude of the scattering vector is given by $q = (4\pi n/\lambda) \sin(\theta/2)$, where n is the refractive index of the solvent, λ is the wavelength of light, and θ is the scattering angle. Measurements were made at five different angles ranging from 50° to 130°.

Dilute Solution Viscometry. The relative viscosities of dilute micellar solutions were measured using a Cannon-Ubbelohde capillary viscometer immersed in a constant-temperature water bath at 25 °C. The sample in the viscometer was equilibrated for 15 min prior to measurement. Capillaries of various diameters were used so that the flow times were sufficiently high to avoid the need for kinetic energy corrections.

Rheology. Rheological measurements were conducted at 25 °C using a Bohlin CS-10 stress-controlled rheometer in a couette geometry (cup of diameter 27.5 mm and bob of diameter 25 mm and height 37.5 mm). Frequency-sweep experiments were performed at a constant stress (chosen in the linear viscoelastic range) over a frequency range of 0.01 to 100 rad/s.

NMR Spectroscopy. NMR measurements were performed at 25 °C on a Bruker AC250 NMR spectrometer (resonance frequency of 250 MHz for ^{1}H) operating in the Fourier transform mode. For NMR measurements, samples were prepared in D_2O (Cambridge Isotopes).

Results and Discussion

1. Phase Behavior Studies. The electrostatic interactions between SDS and PTHC lead to complex phase behavior in aqueous solutions. In the absence of a complete diagram, a pseudo-ternary phase map of the SDS−PTHC−water system can be useful. Figure 1 shows such a phase map in the water-rich corner at 25 °C. Along the binary SDS−water axis, micellar aggregates are formed above

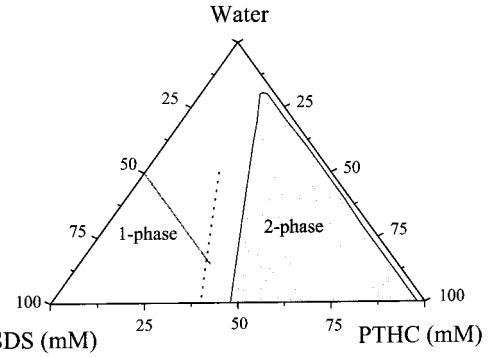

Figure 1. Water-rich corner of the SDS−PTHC−water phase map at 25 °C. Solutions in the one-phase region are unshaded. The solid line indicates the path along which micellar growth is monitored at a fixed SDS concentration. The dashed line indicates the path at a fixed molar ratio of PTHC to SDS ($x_{PTHC} = 0.6$).

the critical micelle concentration (cmc), and the solution is isotropic and of low viscosity. For low SDS concentrations, the solution remains clear and isotropic at all molar ratios of PTHC. At higher SDS concentrations, adding PTHC makes the solutions viscous and, in some cases, viscoelastic (trapped air bubbles recoil). As the molar ratio x_{PTHC} = [PTHC]/[SDS] approaches 1, a turbid precipitate is formed. A two-phase region (shaded) persists at higher PTHC content. Within the two-phase region, the morphology varies: a crystalline precipitate might coexist with an aqueous phase, or the sample might form a turbid dispersion.

Along the binary PTHC−water axis, PTHC is soluble in water over the concentration range studied, and this leaves a narrow one-phase region in the PTHC-rich side. Adding small amounts of SDS to PTHC gives a translucent liquid that eventually transforms into a two-phase mixture of small needlelike crystals and a low-viscosity aqueous phase. The crystals apparently correspond to the equimolar salt of SDS and PTHC.

Interesting phase behavior occurs at higher surfactant and salt concentrations, although the details were not explored. At 150 mM SDS, the addition of PTHC first leads to a viscoelastic phase, then to a biphasic coacervate (two liquid phases in equilibrium), then to a strongly birefringent and turbid phase (possibly a lamellar dispersion), and finally to a precipitate near the equimolar ratio.

This rich phase behavior is a result of strong interactions between the SDS headgroup and the oppositely charged and hydrophobic *p*-toluidinium counterion in PTHC. The counterion tends to adsorb at the micelle−water interface with its aromatic ring intercalated in the hydrophobic interior of the micelle (as will be shown later by NMR spectroscopy). Thus, the counterion forms a 1:1 complex with the surfactant and so reduces the effective charge density at the micelle surface. In turn, there is a shift to microstructures of lower curvature. Note also the similarities between the phase diagram shown here for a surfactant−hydrotrope mixture and those reported for mixtures of cationic and anionic surfactants, e.g., octyl trimethylammonium bromide and SDS.[25] The common feature is strong association between the oppositely charged moieties.

2. Micellar Growth in the Dilute Regime: QLS and Viscosity. QLS was used to probe the variation in micellar size and shape upon addition of PTHC to 50 mM SDS solutions. The average decay rate $\bar{\Gamma}$ from the second-order cumulant expansion of the electric field correlation function $g^1(\tau)$ varies linearly with q^2 (Figure 2). The slope

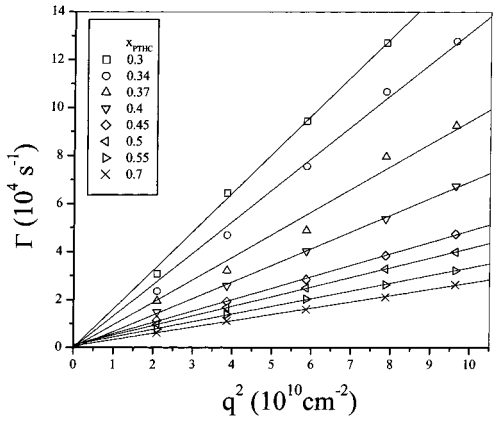

Figure 2. Average decay rates of the intensity correlation function as a function of q^2 for 50 mM SDS with varying molar ratio of PTHC, x_{PTHC}. The corresponding values of x_{PTHC} are shown in the inset.

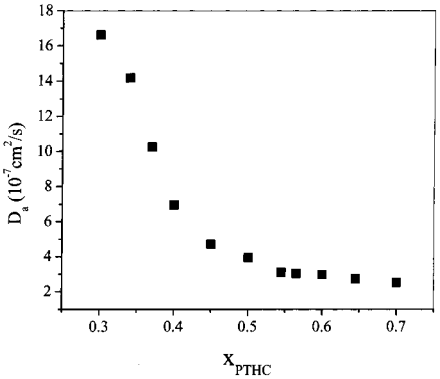

Figure 3. Apparent diffusion coefficient, D_a, for 50 mM SDS as a function of the molar ratio of PTHC, x_{PTHC}.

is the apparent diffusion coefficient D_a of the micelles, and D_a decreases with increasing x_{PTHC} (Figure 3). For $x_{PTHC} \approx 0.3$, D_a is in the range expected for small globular micelles. Upon further addition of PTHC, D_a drops steeply, reflecting a sharp increase in the size of the micelles.

The observed decrease in D_a suggests a transition from spherical micelles to rods of increasing length. We will presently attempt to relate D_a to the average length L of the rods. Note that, in the case of rodlike scatterers, the intensity correlation function can be modified by the coupling between translational and rotational diffusion.[26] Contributions from the rotational diffusion of the rods are expected at large values of qL, typically $qL > 3$, and this would introduce into $\bar{\Gamma}$ a component that is independent of q. Because the plots of $\bar{\Gamma}$ vs q^2 are linear and pass through the origin (Figure 2), D_a depends solely on the translational motion of the micelles.

To extract information about micelle size from D_a, the effect of interactions between neighboring micelles must be taken into account. The apparent diffusion coefficient D_a can be related to the infinite-dilution diffusion coefficient D_0 by

$$D_a = D_0[1 + k_D(c - \mathrm{cmc})] \tag{1}$$

where k_D is the diffusion virial coefficient and c is the surfactant concentration. k_D can be expressed as a competition between an osmotic pressure term that

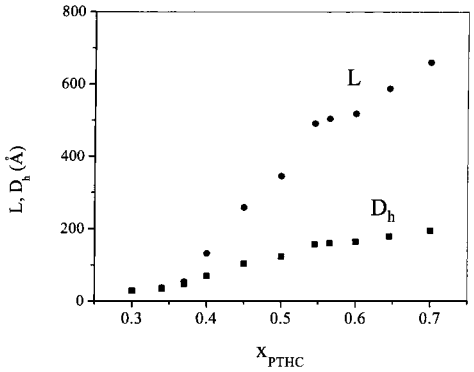

Figure 4. Average length of the rodlike micelle (L) and average equivalent sphere hydrodynamic diameter (D_h) as functions of the molar ratio of PTHC, x_{PTHC}.

enhances the diffusion and a retarding hydrodynamic frictional term.[27] Thus

$$k_D = (2MB_2 - k_f - \bar{v}) \tag{2}$$

where M is the micelle molecular weight, B_2 is the osmotic second virial coefficient, k_f is the hydrodynamic friction virial coefficient, and $\bar{v}$ is the specific volume of the micelle. For a rigid rod[28]

$$B_2 = \left(\frac{\pi N_a d^2 L}{M^2}\right) f \tag{3}$$

where N_a is Avogadro's number, d is the diameter, L is the rod length, and

$$f = \frac{1}{4}\left[1 + \frac{L}{d}\left(1 + \frac{d}{2L}\right)\left(1 + \frac{\pi d}{2L}\right)\right] \tag{4}$$

The hydrodynamic friction virial coefficient k_f for suspensions of uncharged rods is[29]

$$k_f = \left(\frac{RT}{3\eta}\right)\left(\frac{L^2}{D_0 M}\right)\left(\frac{3d}{8L}\right)^{2/3} \tag{5}$$

Finally, the diffusion coefficient D_0 can be related to the length of the rod and its axial ratio $p = L/d$ by Broersma's relationship[30]

$$D_0 = \frac{k_B T}{3\pi\eta L}(\ln p + \zeta) \tag{6}$$

where k_B is the Boltzmann constant, T is the absolute temperature, η is the solvent viscosity, and the shape factor ζ is a function of the axial ratio p. The expressions of Tirado et al., which are valid for axial ratios in the range of 2−30, relate ζ to p[31]

$$\zeta = 0.312 + 0.5656/p - 0.05/p^2 \tag{7}$$

The above expressions allow for the calculation of the diffusion coefficient D_0, and hence the micellar length L, via an iterative procedure, keeping the micelle diameter d at 3.3 nm, which is twice the length of the hydrocarbon chain of SDS. The data (Figure 4) show that the addition of PTHC causes significant micellar growth. A monotonic

(26) Phalakornkul, J. K.; Gast, A. P.; Pecora, R. *Macromolecules* **1999**, *32*, 3122.
(27) Russo, P. S.; Karasz, F. E.; Langley, K. H. *J. Chem. Phys.* **1984**, *80*, 5312.
(28) Isihara, A. *J. Chem. Phys.* **1950**, *18*, 1446.
(29) Peterson, J. M. *J. Chem. Phys.* **1964**, *40*, 2680.
(30) Lehner, D.; Lindner, H.; Glatter, O. *Langmuir* **2000**, *16*, 1689.
(31) Tirado, M. M.; Martinez, C. L.; de La Torre, J. G. *J. Chem. Phys.* **1984**, *81*, 2047.

increase in micellar length L occurs up to ~70 nm (an axial ratio of ~20) at the highest salt content investigated. Thus, the QLS data suggest a transition from spherical micelles to rigid rodlike micelles. The flexibility of the micelles has been neglected in this analysis because their length is expected to be only a few times the persistence length.[24,32]

The consistency of the micellar lengths determined using QLS can be checked by dilute solution viscometry. For a given volume fraction ϕ of suspended rods, the relative viscosity of a dilute colloidal suspension is given by

$$\eta_r = \frac{\eta}{\eta_m} = 1 + \nu\phi + k_1(\nu\phi)^2 \qquad (8)$$

Here, η is the viscosity of the suspension, η_m is the viscosity of the solvent, ν is a shape factor, and k_1 accounts for possible hydrodynamic interactions. The shape factor ν and, hence, η_r are functions of the axial ratio $p = L/d$. In the limit of low p, ν is given by[33]

$$\nu = 2.5 + 0.407(J - 1)^{1.508}, \quad 1 < J < 15 \qquad (9)$$

where $J = p[2/(3 - 1/p)]^{0.5}$ and $k_1 = 0.75$ for prolate ellipsoids.[34] For longer rods in semidilute solution, the effect of multiparticle interactions is captured by the Doi–Edwards model, which gives the following expression for η_r (in the limit, $N > 1/L^3$, N being the number density of the rods)[35]

$$\eta_r = 1 + \frac{3\pi(NL^3)^3}{10\ln\left(\frac{L}{d}\right)} \qquad (10)$$

The number density N of the micelles can be calculated by $N = 4(c - \mathrm{cmc})N_a v_m/(\pi d^2 L)$, where v_m is the volume of the surfactant monomer.

These equations allow for the prediction of η_r for a solution of micelles of a given length. For lengths L such that $N > 1/L^3$, η_r was calculated using eq 10, and for $N < 1/L^3$, η_r was computed using eqs 8 and 9. The values of η_r calculated using the lengths measured by QLS were then compared with experimental measurements of η_r as a function of x_{PTHC} (Figure 5). There is good agreement between the measured and predicted values except at high molar ratios of PTHC. This validates the QLS analysis based on the rigid rod model. Note that the sphere-to-rod transition induced by the addition of PTHC results in a 10-fold increase in η_r. Thus, data for two independently measured quantities, i.e., viscosity and diffusion coefficient, together reveal the growth of micelles upon the addition of PTHC to SDS. This simple analysis takes no account of the length polydispersity of rodlike micelles.

3. Wormlike Micelles in the Semidilute Regime: Rheological Studies. Consider the rheology of SDS/PTHC mixtures at a fixed molar ratio of salt to surfactant, $x_{PTHC} = 0.6$. Figure 6 shows the zero-shear viscosity η_0 as a function of surfactant volume fraction ϕ at $x_{PTHC} = 0.6$ and 25 °C. There is a rapid increase in η_0 by a few orders of magnitude, followed by a maximum in η_0 around $\phi = 0.014$ (i.e., 75 mM). The initial rapid increase in viscosity reflects the exponential growth of the cylindrical micelles at low concentrations. The micelles eventually develop into long, flexible entities and form a transient entangled network, owing to which the system becomes viscoelastic. Dynamic rheological studies were performed on the viscoelastic micellar samples. The relaxation time τ of the system can be estimated from the dynamic frequency spectra as $1/\omega_c$, where ω_c is the frequency at which the dynamic moduli, G' and G'', cross over. For concentrated samples ($\phi > 0.015$), the rheology conforms to the Maxwell model. Accordingly, the storage modulus G' and loss modulus G'' are given by

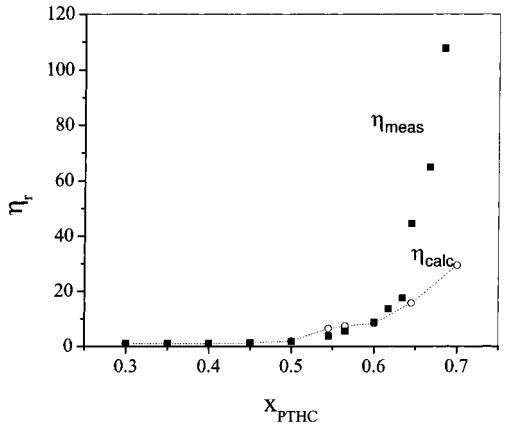

Figure 5. Relative viscosities (η_r) of 50 mM SDS solutions as a function of the molar ratio of PTHC, x_{PTHC}. The circles represent the predictions based on the light scattering data assuming the micelles are rigid rods.

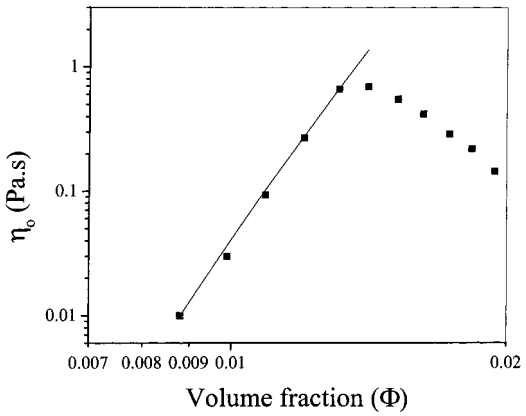

Figure 6. Variation of the zero-shear viscosity, η_0, with surfactant concentration at a fixed molar ratio of PTHC, $x_{PTHC} = 0.6$.

$$G'(\omega) = \frac{G_0\omega^2\tau^2}{1 + \omega^2\tau^2} \quad \text{and} \quad G''(\omega) = \frac{G_0\omega\tau}{1 + \omega^2\tau^2} \qquad (11)$$

where G_0 is the plateau modulus. An alternate estimate of the relaxation time for Maxwell fluids is given by the ratio of the zero-shear viscosity to the plateau modulus, that is, $\tau_M = \eta_0/G_0$.

Figure 7 represents the evolution of the dynamic relaxation time (τ), as well as the ratio of η_0 to G_0 (τ_M), as a function of the surfactant volume fraction ϕ. Both τ and τ_M describe a maximum as a function of ϕ. The two are different at low ϕ but become nearly equal at the higher ϕ values where the sample is a Maxwell fluid. Note that the stress relaxation in an entangled micellar mesh is governed by a competition between two effects. The first is the reptation of the micellar chains with the characteristic time τ_r, and the second is the breaking and recombination of the micelles with the characteristic time τ_b. The samples at volume fractions below the maximum

(32) Magid, L. J. *J. Phys. Chem.* **1998**, *102*, 4064.
(33) Nagarajan, R. *J Colloid Interface Sci* **1982**, *90*, 477.
(34) Matheson, R. R. *Macromolecules* **1980**, *13*, 643.
(35) Doi, M,; Edwards, S. F. *J. Chem. Soc., Faraday Trans. 2* **1978**, *74*, 918.

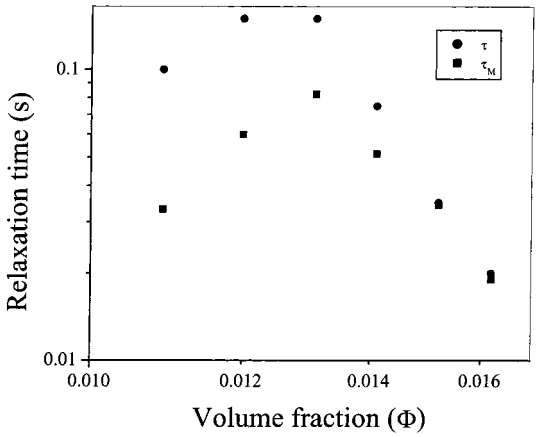

Figure 7. Two measures of the relaxation time, τ and τ_M, as functions of surfactant concentration at a fixed molar ratio of PTHC, $x_{PTHC} = 0.6$.

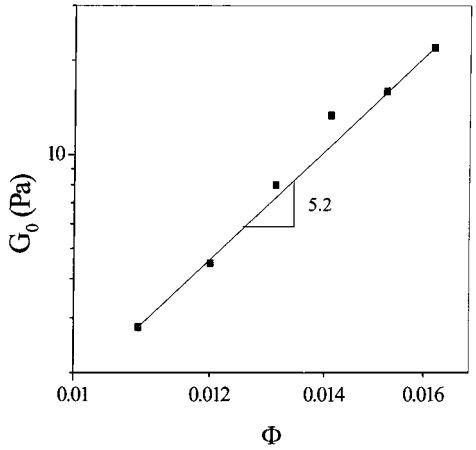

Figure 8. Evolution of the plateau modulus, G_0, as a function of surfactant concentration at a fixed molar ratio of PTHC, $x_{PTHC} = 0.6$.

in Figure 7 show dynamic behavior that is analogous to that of polydisperse polymer solutions, with the stress relaxation being described by a stretched exponential.[23] In that case, $\tau_b \approx \tau_r$. The concentrated regime, on the other hand, is described by the Maxwell model and so corresponds to the fast breaking limit, i.e., $\tau_b \ll \tau_r$. Here, the stress relaxation can be described by a single exponential, and the sample is a Maxwell fluid with the single relaxation time $\tau = \sqrt{\tau_b \tau_r}$.

Figure 8 shows the variation of the plateau modulus G_0 with surfactant volume fraction ϕ at a fixed molar ratio of $x_{PTHC} = 0.6$. G_0 increases monotonically with ϕ in a power-law relationship; however, the observed scaling exponent (5.2) is much higher than that expected for semidilute micellar solutions (2.25). Such a large exponent might reflect the charged nature of the wormlike micelles. Note that the plateau modulus is related to the correlation length ξ for strain fluctuations ($G_0 \approx 1/\xi^3$). The presence of electrostatic interactions increases the range of these correlations, which might suppress the value of G_0 compared to that for uncharged micelles. Indeed, in some charged wormlike micellar systems, the correlation length from rheology ξ is significantly higher than the static correlation length obtained from small-angle neutron scattering (SANS).[36,37] In those samples, with the addition

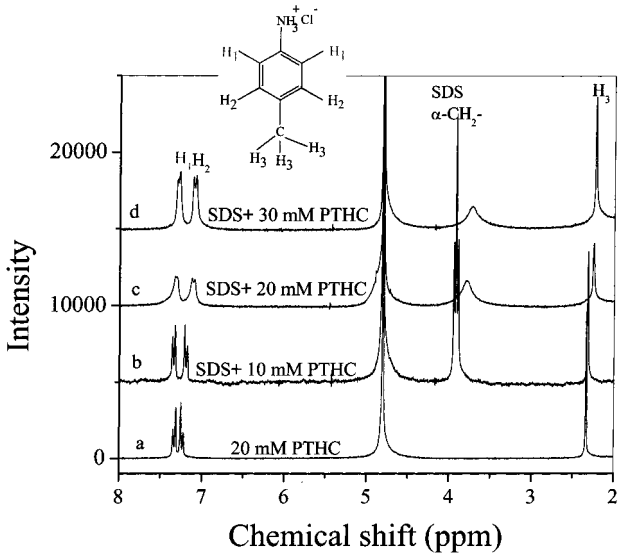

Figure 9. ^{1}H NMR spectra of the salt PTHC and SDS/PTHC mixtures. The SDS concentration in the mixture is kept constant at 50 mM.

of salt, the ξ value from rheology decreases and eventually approaches the value obtained from SANS.[36] Thus, the observed increase in the scaling exponent of G_0 is probably due to the presence of electrostatic interactions.

The notable features of the rheology are the maxima in the relaxation time and the zero-shear viscosity. From the Maxwell relation, $\eta_0 = \tau G_0$, it is clear that the two maxima track each other (as G_0 increases monotonically with ϕ, Figure 8). A possible explanation for the maxima is that it reflects a transition from linear to branched micelles. Branched micelles are expected to show a lower viscosity than linear micelles because they have an additional avenue for stress relaxation (involving the sliding of branch points along the micelle).[38] The question then is why SDS micelles in the presence of PTHC would develop branches. It is true that the insertion of the PTHC hydrotrope into the SDS micelle will likely increase the surfactant packing parameter and decrease the spontaneous curvature of the surfactant monolayer. Thus, the relative energy of formation of highly curved endcaps will increase, endcaps will be less likely to form, and small micelles will grow with added PTHC. At fixed x_{PTHC} and increasing surfactant concentration, it is possible that the increasing density of micelle segments will allow branch formation as the curvature at the branch points will be lower than that at an endcap.

4. Counterion Adsorption and Micellar Dynamics: NMR Studies. The molecular origin of rodlike micelle growth is believed to be the adsorption or insertion of the hydrotrope into the micelle. NMR spectroscopy is an ideal probe of the average position and orientation of counterions on the micellar surface. Past NMR studies of aromatic counterions on cationic micelles showed an upfield shift in proton resonances of the aromatic moiety, from which it was inferred that the aromatic rings inserted into the micelles.[39] Here, proton NMR spectra of PTHC were measured in the presence and absence of SDS (Figure 9). The NMR spectra of 20 mM PTHC in D_2O shows the two ortho protons as a downfield doublet ($\delta = 7.32$ and 7.35 ppm) because of coupling with the meta protons. The two meta protons appear slightly upfield ($\delta = 7.23$ and 7.25

(36) Schmitt, V.; Lequeux , F. *J. Phys. II* **1995**, *5*, 193.
(37) Koehler, R. D.; Raghavan, S. R.; Kaler, E. W. *J. Phys. Chem. B* **2000**, *104*, 11035.
(38) Lequeux, F. *Europhys. Lett.* **1992**, *19*, 675.
(39) Kreke, P. J.; Magid, L. J.; Gee, J. C. *Langmuir* **1996**, *12*, 699.

ppm), again as a doublet. The three methyl protons at the para position are observed at $\delta = 2.33$ ppm.

In the case of 10 mM PTHC in the presence of 50 mM SDS, both the meta protons and the *p*-CH_3 resonances are shifted slightly upfield from their original positions, whereas the positions of the ortho resonances remain practically the same. This clearly indicates that the cationic additive strongly binds to the surface of the micelles with its meta and para positions inserted into the micellar interior and the ortho protons and the NH_3 group protruding from the micelle surface. An extra peak also appears in the spectra, a triplet observed around $\delta = 3.91$ ppm, that arises from the α-CH_2 of the SDS (i.e., the CH_2 that is directly bonded to the O atom of the sulfate headgroup). All other proton resonances of SDS appear below 2 ppm and show no significant changes upon the addition of PTHC except for line broadening effects.

In the case of 20 mM PTHC and 50 mM SDS, the m- and p-proton resonances are shifted further upfield, indicating an increased population of PTHC in the micelles. Furthermore, the resonance lines are broadened and the multiplets can not be resolved, indicating a significantly larger micelle size. The line broadening for the *p*-CH_3 protons is much less than that for the aromatic protons. This indicates that the rotational motion of the hydrotrope is anisotropic, the preferential axis being perpendicular to the micellar surface. Similar effects have been reported for salicylate anions in cationic micelles.[40] Also, the SDS α-CH_2 proton resonances are shifted upfield by the addition of PTHC, further confirming the intercalation of aromatic rings among the SDS headgroups. For 30 mM PTHC and 50 mM SDS, the spectra are similar to the above, except that the m and p protons and the α-CH_2 protons are shifted slightly upfield. Further addition of PTHC causes precipitation of the equimolar salt.

(40) Shikata, T.; Morishima, Y. *Langmuir* **1997**, *13*, 1931.

Conclusions

SDS micelles grow in the presence of a hydrotropic salt PTHC. The phase behavior in the water-rich side of the pseudo-ternary phase diagram resembles that of a typical cationic−anionic mixture, thereby indicating the strong association characteristics of the surfactant and salt. NMR studies confirm the adsorption of the *p*-toluidinium counterion from PTHC onto the micellar surface and show that the aromatic ring is intercalated between the hydrocarbon chains in the interior of the micelle.

The addition of even low concentrations of PTHC to SDS promotes a transition from spherical to rodlike micelles. Consequently, there is a sharp decrease in the translational diffusion coefficient measured by QLS, as well as a dramatic increase in the viscosity of the solutions. Analysis of the QLS data using a rigid-rod model yields the rod length as a function of composition. The dynamic rheological behavior is purely Maxwellian at high surfactant concentrations. At a fixed molar ratio of PTHC to SDS, there are maxima in the zero-shear viscosity and relaxation time as a function of the surfactant concentration. The maxima are possibly due to a transition from linear to branched micelles.

Acknowledgment. Support of this work by the NSF (CTS-9814399) is gratefully acknowledged. P.A.H is thankful to Dr. C. Manohar, IIT, Mumbai, India, for fruitful discussions and to Dr. Steve Bai of the Department of Chemisty, University of Delaware, for help with NMR experiments.

LA011435I